

the occurrence of only terminal and μ_2 -sulfur atoms in the trimer 4.³ The difference is readily attributed to the much smaller steric bulk of the edt ligand.

Acknowledgment. We are grateful to the Natural Sciences and Engineering Research Council of Canada for financial support of this work through grants to P.A.W.D and N.C.P.

Registry No. 1, 86860-88-0.

Supplementary Material Available: Listings of anisotropic thermal parameters, root-mean-square amplitudes of vibration, torsion angles, the weighted least-squares plane, difference Fourier peaks, and structure amplitudes (14 pages). Ordering information is given on any current masthead page.

Contribution from the Department of Chemistry, Gorlaeus Laboratories, State University Leiden, 2300 RA Leiden, The Netherlands

Linear Trinuclear Transition-Metal Compounds Containing 3,5-Diethyl-1,2,4-triazole and Fluoride as Bridging Ligands. X-ray Structure of Bis[(μ -fluoro)bis(μ -3,5-diethyl-1,2,4-triazole- N^1, N^2)bis(thiocyanato- N)(3,5-diethyl-1,2,4-triazole- N^1)cobalt(II)- F, N^1, N^1]cobalt(II) Dihydrate

FREDERIK J. RIETMEIJER, GERARD A. VAN ALBADA, RUDOLF A. G. DE GRAAFF, JAAP G. HAASNOOT, and JAN REEDIJK*

Received February 4, 1985

The synthesis and characterization of three isomorphous trimers containing 3,5-diethyl-1,2,4-triazole are described. The compounds are of general composition $[M_3(\text{detrH})_6(\text{NCS})_4F_2](\text{H}_2\text{O})_2$ ($M = \text{Mn, Co, Ni}$). A single-crystal X-ray analysis of the Co compound shows the presence of a linear trinuclear unit $(\text{SCN})_2(\text{detrH})\text{Co}(\text{detrH})_2\text{FCoF}(\text{detrH})_2\text{Co}(\text{detrH})(\text{NCS})_2$. This compound crystallizes in the monoclinic space group $P2_1/c$ with $a = 8.251$ (2) Å, $b = 20.899$ (3) Å, $c = 17.320$ (4) Å, $\beta = 101.57$ (2)°, and $Z = 2$. The structure was solved by using standard heavy-atom techniques and a local set of programs for automatic crystal structure determination. Conventional least-squares refinement techniques resulted in final residuals $R = 0.032$ and $R_w = 0.043$. Neighboring Co(II) ions in the linear centrosymmetric trinuclear species are linked by two 1,2-bidentate triazole ligands and one bridging fluoride anion. The coordination sphere of the terminal Co(II) ions is completed by two N-bonded thiocyanate anions and one monodentate triazole ligand. The Co...Co distance in the trimer is 3.3726 (3) Å. The Co-F distances are 1.992 (1) and 2.019 (1) Å. The Co-N distances are in the range 2.09–2.21 Å. Fitting of the magnetic data of the Ni trimer according to the isotropic Heisenberg model results in $J = -11.1$ (9) cm^{-1} ($J/k = -16.0$ K) and $g = 2.28$ (1). An expression for the susceptibility of the Co trimer according to the Ising model is derived by assuming an effective spin of $1/2$ for Co and neglecting χ_{\perp} . Fitting of the magnetic data of the Co compound to the expression obtained yields $J_1 = -17.4$ (7) cm^{-1} and $g_1 = 8.23$ (4). The magnetic properties of the fluoride-bridged trimers are compared to magnetic data of closely related compounds containing N-bridging isothiocyanato ligands instead of fluoride anions.

Introduction

Current research activity concerning the structural and magnetic properties of polynuclear transition-metal compounds is aimed at understanding the structural and chemical features governing magnetic exchange coupling through small bridging ligands. The literature on this subject is exhaustive, mainly dealing with dimeric compounds¹⁻⁶ and chains.⁷⁻⁹ Linear trinuclear compounds for which structural and magnetic information is available are documented to a limited extent.¹⁰⁻¹⁵ Recently it was reported¹⁶ linear

trinuclear compounds are formed when transition-metal thiocyanates are reacted with 3,5-dialkyl-1,2,4-triazoles; neighboring metal ions (Co, Mn, Ni) in the linear array are linked by two 1,2-bidentate triazole ligands and one N-bridging isothiocyanato ligand. It was suggested that the double-triazole-bridging framework should also allow incorporation of anions other than thiocyanate, e.g., fluoride or hydroxide: such changes are interesting because changing the bridging anion might be a powerful tool in tuning the magnetic properties of these systems. The crystal structure now reported of $[\text{Co}_3\text{F}_2(\text{detrH})_6(\text{NCS})_4](\text{H}_2\text{O})_2$ proves that incorporation of fluoride anion is possible; moreover, magnetic susceptibility data of both the Ni and the Co trimers in the 4–80 K region reveal quite substantial differences between the exchange constants of the fluoride-bridged and isothiocyanate-bridged compounds. In the present study we try to account for these differences in a qualitative way by comparison of the M-X-M

- (1) Hay, P. J.; Thibeault, J. C.; Hoffmann, R. *J. Am. Chem. Soc.* **1975**, *97*, 4884 and references cited therein.
- (2) Kahn, O. *Inorg. Chim. Acta* **1982**, *62*, 1.
- (3) Marsh, W. E.; Hatfield, W. E.; Hodgson, D. J. *Inorg. Chem.* **1982**, *21*, 2679.
- (4) Marsh, W. E.; Bowman, T. L.; Harris, C. S.; Hatfield, W. E.; Hodgson, D. J. *Inorg. Chem.* **1981**, *20*, 3864.
- (5) Marsh, W. E.; Patel, K. C.; Hatfield, W. E.; Hodgson, D. J. *Inorg. Chem.* **1983**, *22*, 511 and references cited therein.
- (6) Sikorav, S.; Bkouche-Waksman, I.; Kahn, O. *Inorg. Chem.* **1984**, *23*, 490 and references cited therein.
- (7) van Ooijen, J. A. C.; Reedijk, J. *Inorg. Chim. Acta* **1977**, *25*, 131.
- (8) Hatfield, W. E.; Weller, R. R.; Hall, J. W. *Inorg. Chem.* **1980**, *19*, 3825.
- (9) Boyd, P. D. W.; Mitra, S.; Raston, C. L.; Towbottom, G. L.; White, A. H. *J. Chem. Soc., Dalton Trans.* **1981**, 13.
- (10) de Meester, P.; Skapski, A. C. *J. Chem. Soc., Dalton Trans.* **1972**, 2400.
- (11) Brown, D. B.; Wasson, J. A.; Hall, J.; Hatfield, W. E. *Inorg. Chem.* **1977**, *16*, 2526.
- (12) Banci, L.; Bencini, A.; Gatteschi, D. *Inorg. Chem.* **1983**, *22*, 2681.

- (13) Baker, W. A.; Helm, F. T. *J. Am. Chem. Soc.* **1975**, *97*, 2295.
- (14) (a) Matsumoto, N.; Nishida, Y.; Kida, S.; Ueda, I. *Bull. Chem. Soc. Jpn.* **1976**, *49*, 117. (b) Nishida, Y.; Kida, S. *Chem. Lett.* **1974**, 339.
- (15) (a) Vos, G.; le Febvre, R. A.; de Graaff, R. A. G.; Haasnoot, J. G.; Reedijk, J. *J. Am. Chem. Soc.* **1983**, *105*, 1682. (b) Groeneveld, L. R.; Vos, G.; le Febvre, R. A.; de Graaff, R. A. G.; Haasnoot, J. G. *Inorg. Chim. Acta*, in press. (c) Vos, G.; Haasnoot, J. G.; Schaminee, P. L. M.; Verschoor, G. C.; Reedijk, J., submitted for publication in *Inorg. Chim. Acta*. (d) Vos, G.; de Graaff, R. A. G.; Haasnoot, J. G.; van der Kraan, A. M.; de Vaal, P.; Reedijk, J. *Inorg. Chem.* **1984**, *23*, 2905.
- (16) van Albada, G. A.; de Graaff, R. A. G.; Haasnoot, J. G.; Reedijk, J. *Inorg. Chem.* **1984**, *23*, 1404.

Table I. Crystal and Diffraction Data of $[\text{Co}_3\text{F}_2(\text{detrH})_6(\text{NCS})_4](\text{H}_2\text{O})_2$

cryst color	red
cryst habit	rod shape
M_r	1234.2
space group ^a	$P2_1/c$
a , Å	8.251 (2)
b , Å	20.899 (3)
c , Å	17.320 (4)
β , deg	101.57 (2)
V , Å ³	2926
Z	2 (trimers)
D_{measd}^b , Mg·m ⁻³	1.39 (1)
D_{calcd} , Mg·m ⁻³	1.40
$F(000)$	1269.4
θ range, deg	2–27
octants colled	$k > 0, l > 0$
no. of measd reflns	6773
no. of independent reflns	6561
no. of significant reflns ($I > 2\sigma(I)$)	4185
agreement factor between equiv reflns	0.024
data collcn temp	room temp
radiation used ^c	Mo K α
diffractometer type	Enraf-Nonius CAD-4
μ , cm ⁻¹ ^d	10.72
final R value ($\sum F_o - F_c /\sum F_o $)	0.032
final R_w value ($[\sum w(F_o - F_c)^2/\sum w F_o ^2]^{1/2}$)	0.043
transmissn range (azimuth scan)	0.97–1.03

^aDetermined unambiguously from systematic absence of reflections.

^bMeasured by flotation in $\text{CHCl}_3/\text{EtOH}$. ^cGraphite monochromatized. ^dThe data were not corrected for absorption.

bridging angles (X is the bridging anion).

Experimental Section

Starting Materials. Metal(II) thiocyanates were freshly prepared or generated in situ from commercially available metal(II) nitrates and ammonium thiocyanate. Both commercially available metal(II) fluorides and metal(II) tetrafluoroborates (obtained from commercially available metal(II) carbonates and hydrofluoroboric acid) could be used as a source of fluoride anions. The synthesis of 3,5-diethyl-1,2,4-triazole was described earlier.¹⁶

Syntheses of the Coordination Compounds. Two different methods were used for the synthesis of the trimeric products.

Method 1. Ligand-Induced Decomposition of the Metal(II) Tetrafluoroborate¹⁷ in the Presence of Metal(II) Thiocyanate ($M = \text{Co}, \text{Mn}, \text{Ni}$). A mixture of 2.5 mmol of metal(II) tetrafluoroborate, 5.0 mmol of metal(II) nitrate, and 10 mmol of ammonium thiocyanate was dissolved in 20 mL of water, and the ligand solution (20 mmol in 20 mL of water) was added slowly to this mixture. After the solution was allowed to stand at room temperature, the trimeric compound $[\text{Co}_3\text{F}_2(\text{detrH})_6(\text{NCS})_4](\text{H}_2\text{O})_2$ slowly crystallized. In the case of Mn only a small quantity of product could be isolated after partial evaporation of the solvent.

Method 2. Reaction of Metal(II) Fluoride with the Ligand Followed by Addition of Metal Thiocyanate Solution. A mixture of 2.5 mmol of metal(II) fluoride and 20 mmol of detrH was dissolved in 25 mL of boiling water, the solution was filtered to remove some insoluble material, and a solution of metal(II) thiocyanate (5.0 mmol in 20 mL of water) was added slowly. The products crystallized on standing at room temperature; the Mn compound again crystallized after concentration of the reaction mixture. Changing the ratio $\text{MF}_2:\text{M}(\text{NCS})_2:\text{detrH}$ to 1:2:2 or 1:1:2 did not seem to affect the composition of the product.

Physical and Analytical Measurements. Metal analyses were performed by using standard EDTA titration techniques. C, H, N, S, and F analyses were carried out by the Microanalytical Laboratory of University College, Dublin, Republic of Ireland, and by the Microanalytical Laboratory of Dr. Pascher, Bonn, Germany. Infrared spectra were obtained as Nujol mulls and as KBr pellets (4000–200 cm^{-1}) on a Perkin-Elmer 580 spectrophotometer. Ligand field spectra were obtained by the diffuse-reflectance method on the solid powders. Magnetic susceptibility measurements in the 4–80 K region were carried out with a PAR vibrating-sample magnetometer equipped with a Janis-type cryostat.

Table II. Fractional Coordinates of Non-Hydrogen Atoms ($\times 10^4$) in $[\text{Co}_3(\text{detrH})_6\text{F}_2(\text{NCS})_4](\text{H}_2\text{O})_2$, with Their Esd's in Parentheses

atom	x/a	y/b	z/c
Co(1) ^a	0	0	0
Co(2)	-1086.4 (4)	251.8 (2)	1751.5 (2)
F	-1670 (2)	-149.3 (7)	688.3 (8)
O	380 (4)	3295 (1)	481 (1)
N(1)	-3407 (3)	654 (1)	1746 (2)
C(1)	-4551 (4)	975 (2)	1711 (2)
S(1)	-6131 (1)	1455.7 (5)	1653.0 (7)
N(2)	-1705 (3)	-569 (1)	2326 (2)
C(2)	-2248 (3)	-1030 (2)	2527 (2)
S(2)	-3100 (1)	-1683.8 (4)	2802.4 (6)
N(11)	22 (3)	968 (1)	400 (1)
N(21)	-508 (3)	1086 (1)	1100 (1)
C(31)	-552 (3)	1708 (1)	1184 (2)
N(41)	-47 (3)	1992 (1)	574 (1)
C(51)	307 (3)	1520 (1)	100 (2)
C(31A)	-1082 (4)	2073 (1)	1833 (2)
C(31B)	-2433 (5)	2544 (2)	1539 (2)
C(51A)	913 (4)	1625 (1)	-647 (2)
C(51B)	-304 (5)	1971 (2)	-1268 (2)
N(12)	1836 (3)	-229 (1)	1032 (1)
N(22)	1358 (3)	-178 (1)	1756 (1)
C(32)	2480 (3)	-470 (1)	2281 (2)
N(42)	3670 (3)	-696 (1)	1927 (1)
C(52)	3250 (3)	-539 (1)	1150 (2)
C(32A)	2468 (4)	-568 (2)	3128 (2)
C(32B1) ^b	406 (4)	-42 (3)	368 (2)
C(32B2) ^b	397 (2)	-27 (2)	365 (1)
C(52A)	4245 (4)	-695 (2)	550 (2)
C(52B)	4442 (4)	-1410 (2)	439 (2)
N(13)	65 (3)	741 (1)	2837 (1)
N(23)	1525 (3)	1061 (1)	2890 (1)
C(33)	1933 (4)	1351 (2)	3581 (2)
N(43)	803 (4)	1223 (1)	4004 (2)
C(53)	-312 (4)	850 (2)	3530 (2)
C(33A)	3426 (5)	1774 (2)	3798 (2)
C(33B1) ^b	406 (2)	185.7 (6)	469.2 (7)
C(33B2) ^b	449 (3)	163 (1)	462 (1)
C(53A1) ^b	-171 (3)	50 (1)	378 (2)
C(53A2) ^b	-192 (2)	66.2 (7)	374 (1)
C(53B1) ^b	-265 (2)	101.4 (7)	410.6 (8)
C(53B2) ^b	-169 (1)	21.6 (5)	442.2 (5)

^aSpecial position. ^bMultiplication factor 10^3 .

X-ray Data Collection and Refinement. A red monoclinic crystal of $[\text{Co}_3\text{F}_2(\text{detrH})_6(\text{NCS})_4](\text{H}_2\text{O})_2$ (dimensions $0.50 \times 0.32 \times 0.28 \text{ mm}^3$) was mounted and used for the data collection. Crystallographic data and relevant information on the data collection and refinement have been summarized in Table I. The data were corrected for Lorentz and polarization effects, but not for absorption. Scattering factors, including anomalous dispersion, were taken from ref 18. The cobalt positions, located in a Patterson synthesis, were used as input data for AUTOFOR, a program for automatic crystal structure determination developed in our laboratory.¹⁹ All non-hydrogen atomic positions were obtained in this way. Hydrogen atom positions were, if possible, located by subsequent least-squares refinement cycles followed by difference Fourier syntheses. The refinement was carried out by using weights $1/\sigma^2(F)$, with $\sigma(F) = \sigma(F)/(\text{counting statistics}) + 0.03F$. The positional and thermal parameters of the hydrogen atoms located were not refined (the B_{iso} values were fixed at the initial B_{iso} value of the corresponding mother atom). Some of the ethyl groups, in particular those of the terminal triazole ligands, appeared to have rather large isotropic thermal parameters that may be ascribed to disorder. Therefore, where appropriate, two alternative positions for ethyl group carbon atoms were used in the refinement. Waser constraints²⁰ were used to refine the atomic positions of these atoms: $\text{C}(32)-\text{C}(32\text{A}) = \text{C}(33)-\text{C}(33\text{A}) = \text{C}(53)-\text{C}(53\text{A}1) = \text{C}(53)-\text{C}(53\text{A}2) = 1.495 \text{ \AA}$ ($\sigma = 0.02 \text{ \AA}$); $\text{C}(32\text{A})-\text{C}(32\text{B}1) = \text{C}(32\text{A})-\text{C}(32\text{B}2) = \text{C}(33\text{A})-\text{C}(33\text{B}1) = \text{C}(33\text{A})-\text{C}(33\text{B}2) = \text{C}(53\text{A}1)-\text{C}(53\text{B}1) = \text{C}(53\text{A}2)-\text{C}(53\text{B}2) = 1.520 \text{ \AA}$ ($\sigma = 0.02 \text{ \AA}$); $\text{C}(32)-\text{C}(32\text{A})-\text{C}(32\text{B}1) = \text{C}(32)-\text{C}(32\text{A})-\text{C}(32\text{B}2) = \text{C}(53)-\text{C}($

(17) Reedijk, J.; ten Hoedt, R. W. M. *Recl.: J. R. Neth. Chem. Soc.* **1982**, 101, 49.

(18) "International Tables for X-ray Crystallography"; Kynoch Press: Birmingham, England, 1974; Vol. 4.

(19) Kinneving, A. J.; de Graaff, R. A. G. *J. Appl. Crystallogr.* **1984**, 17, 364.

(20) Waser, J. *Acta Crystallogr.* **1963**, 16, 1091.

Table III. Colors, X-ray Type, and Infrared and Ligand-Field Data of $[M_3(\text{detrH})_6F_2(\text{NCS})_4](\text{H}_2\text{O})_2^a$

metal	color	X-ray type ^b	M-F, cm^{-1}	ν_{CN} , cm^{-1}	ligand field, 10^3 cm^{-1}
Mn	pink	A	335, 385	2080 (b)	
Co	red	A	350, 385	2085, 2105	9.3, 15.9 (sh), 20.1
Ni	blue	A	370, 400	2105, 2120	10.0, 13.6 (w), 16.6, 26.9

^aM = Co, Ni, Mn; b = broad, w = weak, sh = shoulder. ^bFrom powder diffraction measurements.

Table IV. Relevant Bond Lengths (Å) and Bond Angles (deg) in $[\text{Co}_3(\text{detrH})_6F_2(\text{NCS})_4](\text{H}_2\text{O})_2$, with Their Esd's in Parentheses^a

Co(1)---Co(2)	3.3726 (3)	Co(1)-N(11)	2.137 (2)
Co(1)-F	2.019 (1)	Co(1)-N(12)	2.152 (2)
Co(2)-F	1.992 (1)	Co(2)-N(13)	2.183 (2)
Co(2)-N(1)	2.090 (3)	Co(2)-N(21)	2.181 (2)
Co(2)-N(2)	2.096 (3)	Co(2)-N(22)	2.206 (2)
N(1)-C(1)	1.149 (4)	N(2)-C(2)	1.147 (4)
C(1)-S(1)	1.633 (3)	C(2)-S(2)	1.650 (3)
Co(1)-F-Co(2)	114.44 (7)	Co(2)-N(21)-N(11)	116.7 (2)
Co(1)-N(11)-N(21)	117.9 (2)	Co(2)-N(22)-N(12)	116.9 (2)
Co(1)-N(12)-N(22)	116.8 (2)	Co(2)-N(13)-N(23)	120.9 (2)
Co(2)-N(1)-C(1)	167.7 (3)	Co(2)-N(2)-C(2)	168.4 (3)
F-Co(1)-N(11)	94.77 (7)	F-Co(1)-N(11)'	85.23 (7)
F-Co(1)-N(12)	85.73 (7)	F-Co(1)-N(12)'	94.27 (7)
F-Co(2)-N(21)	83.97 (7)	F-Co(2)-N(22)	83.31 (7)
N(12)-Co(1)-N(11)	91.02 (8)	N(12)-Co(1)-N(11)'	88.98 (8)
N(1)-C(1)-S(1)	177.7 (3)	N(2)-C(2)-S(2)	177.9 (3)

^aPrimed atoms are generated by the symmetry operation $-x, -y, -z$.

(53A1)-C(53B1) = C(53)-C(53A2)-C(53B2) = 110.2° ($\sigma = 2.7^\circ$). Initially used constraints, based on ideal tetrahedral geometry, did not yield satisfactory refinement results. Because one of the anisotropic thermal parameters of the water oxygen atom was rather large, two alternative positions were taken into account in an early stage of the refinement. However, the two separate positions merged into the initial oxygen position in a later stage. The final R value was 0.032 for 4185 significant reflections. Atomic positions of the non-hydrogen atoms are listed in Table II. Listings of F_{obsd} and F_{calcd} values, hydrogen atom positions, and the thermal parameters of the non-hydrogen atoms are available.²¹

Results and Discussion

General Considerations. Notwithstanding the use of several $\text{MF}_2:\text{M}(\text{NCS})_2:\text{detrH}$ ratios (vide supra), only the compounds listed in Table III could be isolated. The results of elemental analyses (metal, C, H, N, F, S) are satisfactory. The synthetic procedures described above are not successful in the case of $M = \text{Cu}$. Except for the far-IR region, the infrared spectra of the Mn, Co, and Ni compounds are essentially similar. X-ray powder patterns of the three compounds are also similar, suggesting their basic structure is identical.

Molecular Structure of $[\text{Co}_3(\text{detrH})_6F_2(\text{NCS})_4](\text{H}_2\text{O})_2$. The centrosymmetric trimeric unit is shown in Figure 1, together with the atomic labeling scheme used. Relevant bond lengths and angles are listed in Table IV. Bond distances and angles of the triazole rings are given as supplementary material.²¹

The central cobalt ion is octahedrally surrounded by four bridging triazole ligands and two fluoride anions. The octahedron is compressed along the F-Co-F' axis, given the distances Co(1)-F = 2.019 (1) Å, Co(1)-N(11) = 2.137 (2) Å, and Co(1)-N(12) = 2.152 (2) Å. The coordination geometry of the terminal cobalt ions is also (distorted) octahedral; apart from two bridging triazole nitrogens (at distances Co(2)-N(21) = 2.181 (2) Å and Co(2)-N(22) = 2.206 (2) Å) and a fluoride anion (Co(2)-F = 1.992 (1) Å), two terminal thiocyanate ligands (at distances Co(2)-N(1) = 2.090 (3) Å and Co(2)-N(2) = 2.096 (3) Å) and one monodentate triazole ligand (Co(2)-N(13) = 2.183 (2) Å) are present. The Co---Co distance in the trimer is 3.3726 (3) Å. The terminal

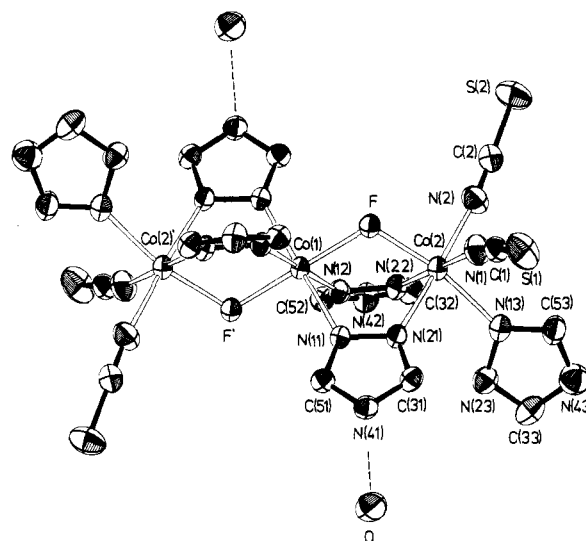


Figure 1. ORTEP drawing of $[\text{Co}_3(\text{detrH})_6F_2(\text{NCS})_4](\text{H}_2\text{O})_2$, showing the atomic labeling scheme, the positions of the water molecules relative to the ligands, and the intramolecular hydrogen bonds (dotted lines). Primed atoms are generated by the center of symmetry. Ethyl groups of triazole ligands have been omitted for clarity. The numbering of the ethyl groups as mentioned in Table II is as follows: C(3nA) and C(3nB) are attached to C(3n); C(5nA) and C(5nB), to C(5n) (where n denotes the number of the ring). Disordered positions have been given the labels 1 and 2 (e.g., C(32B1) and C(32B2) are both attached to C(32A)).

Table V. Hydrogen-Bonding Distances (Å) and Angles (deg) in $[\text{Co}_3(\text{detrH})_6F_2(\text{NCS})_4](\text{H}_2\text{O})_2$, with Their Esd's in Parentheses

O...N(41)	2.755 (3)	O...H(41)-N(41)	169.3 (2)
O...S(2)'	3.346 (3) ^a	O-H(O2)...S(2)'	160.9 (2)
O...N(43)''	2.835 (3) ^b	O-H(O1)...N(43)''	167.7 (2)
S(1)...N(23)'''	3.267 (3) ^c	S(1)...H(23)'''-N(23)'''	152.1 (2)
S(2)...N(42)'''	3.471 (2)	S(2)...H(42)'''-N(42)'''	165.4 (2)

^aAtoms with single primes are generated by the symmetry operation $-x, 1/2 + y, 1/2 - z$. ^bAtoms with double primes are generated by $x, 1/2 - y, -1/2 + z$. ^cAtoms with triple primes are generated by $-1 + x, y, z$.

thiocyanate anions are coordinated in an almost linear fashion, as is indicated by the angles Co(2)-N(1)-C(1) = 167.7 (3)° and Co(2)-N(2)-C(2) = 168.4 (3)°. The bridging angle Co(1)-F-Co(2) is 114.44 (7)°. Hydrogen bonding is important for the stabilization of the structure. Hydrogen-bond distances and angles are given in Table V. Hydrogen bonds exist between the water molecule and an NH nitrogen atom of a bridging triazole ligand (O...N(41) = 2.755 (3) Å; O...H(41)-N(41) = 169.3 (2)°); the OH oxygen atoms are involved in intermolecular hydrogen-bonding contacts with thiocyanate sulfur (O...S(2)' = 3.346 (3) Å; O-H(O2)...S(2)' = 160.9 (2)°) and with a noncoordinating nitrogen atom of a terminal triazole ligand (O...N(43)'' = 2.835 (3) Å; O-H(O1)...N(43)'' = 167.7 (2)°). The thiocyanate anions are also involved in intermolecular hydrogen bonds of intermediate strength with N-H atoms of terminal and bridging triazole ligands, as is illustrated by the distances S(1)...N(23)''' = 3.267 (3) Å (S(1)...H(23)'''-N(23)''' = 152.1 (2)°) and S(2)...N(42)''' = 3.471 (2) Å (S(2)...H(42)'''-N(42)''' = 165.4 (2)°).

Spectroscopic and Magnetic Properties. As may be expected for a series of isomorphous compounds, the IR spectra of the Co, Ni, and Mn trimers are almost identical. Some characteristic features are given in Table III. The vibration bands with doublet character around 2100 cm^{-1} can be assigned to ν_{CN} stretchings of the terminal N-bonded thiocyanate ligands²²⁻²⁴ (in the case of

- (22) Groeneveld, L. R.; Vos, G.; Verschoor, G. C.; Reedijk, J. *J. Chem. Soc., Chem. Commun.* **1982**, 620.
 (23) Cotton, F. A.; Davison, A.; Ilsley, W. H.; Trop, H. S. *Inorg. Chem.* **1979**, *18*, 2719.
 (24) Drew, M. G. B.; Esho, F. S.; Nelson, S. M. *Inorg. Chim. Acta* **1983**, *76*, L269.

Table VI. Magnetic Susceptibility Data for $[\text{Co}_3(\text{detrH})_6\text{F}_2(\text{NCS})_4](\text{H}_2\text{O})_2$ and $[\text{M}_3(\text{detrH})_6(\text{NCS})_6](\text{H}_2\text{O})_2$ ($\text{M} = \text{Ni}, \text{Co}$)

compd	$\mu_{\text{eff}}(80 \text{ K}), \mu_{\text{B}}$	θ, K	g	J, cm^{-1}	$J/k, \text{K}$
$\text{Ni}_3(\text{detrH})_6\text{F}_2(\text{NCS})_4(\text{H}_2\text{O})_2$	2.70 (5)	-55 (2)	2.28 (1)	-11.1 (9)	-16 (1)
$\text{Co}_3(\text{detrH})_6\text{F}_2(\text{NCS})_4(\text{H}_2\text{O})_2$	4.01 (5)	-67 (2)	8.23 (4) ^b	-17.4 (7) ^b	-25 (1) ^b
$\text{Co}_3(\text{detrH})_6\text{F}_2(\text{NCS})_4(\text{H}_2\text{O})_2$	4.01 (5)	-67 (2)	4.76 (2) ^c	-13.2 (5) ^c	-19.0 (7) ^c
$\text{Ni}_3(\text{detrH})_6(\text{NCS})_6(\text{H}_2\text{O})_2^a$	3.50 (5)	+14 (4)	2.20 (1)	+9.6 (1)	+13.8 (1)
$\text{Co}_3(\text{detrH})_6(\text{NCS})_6(\text{H}_2\text{O})_2^a$	4.60 (5)	-20 (2)	5.16 (3) ^c	-4.7 (3) ^c	-6.8 (4) ^c

^aThe data are taken from ref 16. ^bDetermined for an Ising trimer $S' = 1/2$. ^cDetermined for a Heisenberg trimer $S' = 1/2$.

Mn, the splitting is less pronounced and a broad band is observed). In all compounds, the ν_{CS} stretching and δ_{NCS} bending vibrations are observed near 790 and 470 cm^{-1} , respectively.²⁵ Because of the small mass of the fluorine atom compared to other ligands, M-F vibrations are usually observed at higher frequencies than other metal-ligand vibrations (the difference is less pronounced, however, in compounds containing fluoride as bridging ligand¹⁷). All three compounds show two distinct vibrations in the 300–400- cm^{-1} region that can be assigned to M-F vibrations (Table III). The observed M-F stretching frequencies are close to the values observed for $\text{MF}_2(\text{dmpz})_2$ chain compounds¹⁷ ($\text{dmpz} = 3,5\text{-dimethylpyrazole}$). The Irving-Williams sequence is obeyed. Ligand field data of the Co and Ni compounds (Table III) are in agreement with an octahedral coordination geometry for the metal ions;^{26,27} the unresolved splitting of the broad absorption band at 20 100 cm^{-1} for the Co compound probably arises from deviations from ideal octahedral geometry of the terminal Co ions (this is clearly indicated by the crystal structure).

The Ni and the Co compounds were also studied by magnetic susceptibility measurements in the 4–80 K region. Magnetic data are given in Table VI. Unfortunately, magnetic data of the isomorphous Mn trimer are not available because not enough product could be isolated.

Several reports dealing with the magnetic behavior of Ni trimers have already been published.^{28–32} The magnetic exchange interactions in centrosymmetric trimers are usually described by the isotropic Hamiltonian $H = -2J[(S_1 \cdot S_2) + (S_2 \cdot S_3)] - 2J_{13}(S_1 \cdot S_3)$, where J and J_{13} represent the exchange constants between neighboring and terminal metal ions, respectively. The Zeeman part of the Hamiltonian ($g\mu_{\text{B}}H(S_1 + S_2 + S_3)$), describing the interaction of the spin system with the magnetic field applied, is then neglected. In the absence of a clearly defined exchange pathway between the terminal Ni ions, J_{13} was taken as zero.^{16,29,31} The spectroscopic splitting constant g was assumed to be equal for all the individual ions, and zero-field splittings and intercluster interactions were assumed to be negligible. Under these conditions, the magnetic susceptibility per mole of Ni ions is calculated as^{28,29}

$$\chi = \frac{2N_{\text{A}}g^2\mu_{\text{B}}^2}{9kT} \frac{3 + 4e^{4x} + 18e^{-2x} + 15e^{2x} + 3e^{-6x}}{3 + 7e^{4x} + 8e^{-2x} + 5e^{2x} + 3e^{-6x} + e^{-4x}} \quad (1)$$

where N_{A} is Avogadro's number, μ_{B} is the Bohr magneton, and $x = J/kT$. The validity of this equation is easily checked by inserting into it the simple "spin-only" case, where no exchange interactions occur, i.e., $x = 0$, reducing the equation to the Curie law, $\chi_{\text{A}} = N_{\text{A}}g^2\mu_{\text{B}}^2S(S + 1)/3kT$ ($S = 1$). Contributions of diamagnetic susceptibility and temperature-independent paramagnetism were introduced as minor corrections to χ_{A} (Figure

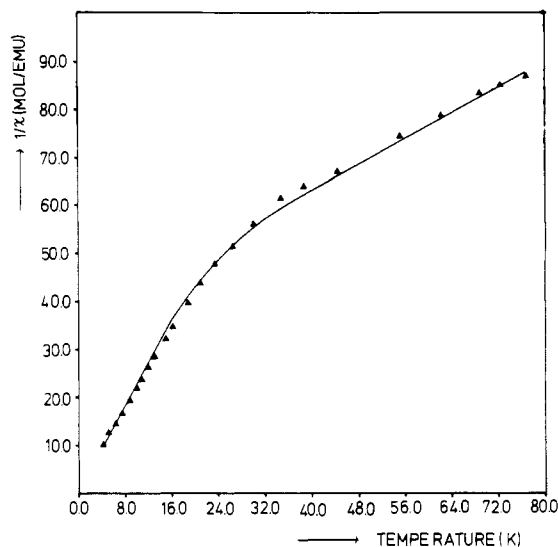


Figure 2. Plot of the reciprocal magnetic susceptibility ($1/\chi$) vs. temperature for $[\text{Ni}_3(\text{detrH})_6\text{F}_2(\text{NCS})_4](\text{H}_2\text{O})_2$. The drawn curve is the theoretical prediction of a linear Heisenberg trimer ($S = 1$) with $g = 2.28$ (1) and $J = -11.1$ (9) cm^{-1} (diamagnetic correction = -223×10^{-6} emu, TIP = 200×10^{-6} emu/Ni).

2). The function minimized in the least-squares-fitting procedure is $\sum w_i(\chi_{\text{obsd}}^i - \chi_{\text{calcd}}^i)^2$; setting weights $w_i = 1$ and allowing J and g to vary simultaneously yield $J = -11.1$ (9) cm^{-1} ($J/k = -16.0$ K) and $g = 2.28$ (1) (Table VI). In Figure 2, the reciprocal susceptibility is shown as a function of temperature (4–80 K). The solid curve is the theoretical prediction of $1/\chi$ according to eq 1. The change in slope in the region $1.5 < kT/|J| < 2$ (for $S = 1$) is characteristic of linear trimers with an antiferromagnetic exchange interaction between nearest neighbors. As Figure 2 shows, the agreement with theory is quite acceptable. Unfortunately, interpretation of the magnetic data of the Co trimer is fundamentally less straightforward on several counts: (1) For the Ni(II) ion in a distorted octahedral environment, the spin-1 approximation holds up to room temperature. In contrast, the Co(II) ion in such an environment may be treated by using a spin- $1/2$ approximation, but only at lower temperatures. (2) The Co(II) ion generally shows appreciable anisotropy, with rather complicated g factors related to the breakdown of the effective spin- $1/2$ approach above. Therefore, a simple Heisenberg type of Hamiltonian is unlikely to be adequate.³⁴ If one assumes, as a first approximation, an Ising type interaction between the Co ions and also an effective spin of $1/2$, a spin Hamiltonian for the Co trimer may be set up:³⁵ $H = -2J(S_{1z}S_{2z} + S_{2z}S_{3z}) - 2J_{13}S_{1z}S_{3z} + g\mu_{\text{B}}H_z(S_{1z} + S_{2z} + S_{3z})$, where $J = J_{12} = J_{23}$. Taking J_{13} as zero and taking into account the eight possible spin states of the trimer (the spins can only be up or down with respect to the z axis), we calculated the eigenvalues as follows: $-J_{\parallel} + 3/2g_{\parallel}\mu_{\text{B}}H_z$; $-J_{\parallel} - 3/2g_{\parallel}\mu_{\text{B}}H_z$; $1/2g_{\parallel}\mu_{\text{B}}H_z$ (twice); $-1/2g_{\parallel}\mu_{\text{B}}H_z$ (twice); $J_{\parallel} + 1/2g_{\parallel}\mu_{\text{B}}H_z$; $J_{\parallel} - 1/2g_{\parallel}\mu_{\text{B}}H_z$. The \parallel signs are added to indicate clearly that we are calculating the parallel susceptibility. Substitution of these

(25) Vos, G. Ph.D. Thesis, Leiden, 1983.

(26) Reedijk, J.; Driessen, W. L.; Groeneveld, W. L. *Recl. Trav. Chim. Pays-Bas* **1969**, *88*, 1095.

(27) Reedijk, J.; van Leeuwen, P. W. N. M.; Groeneveld, W. L. *Recl. Trav. Chim. Pays-Bas* **1968**, *87*, 129.

(28) Long, G. J.; Lindner, D.; Lindvedt, R. L.; Guthrie, J. W. *Inorg. Chem.* **1982**, *21*, 1431.

(29) Ginsberg, A. P.; Martin, R. L.; Sherwood, R. C. *Inorg. Chem.* **1968**, *7*, 932.

(30) Boyd, P. D. W.; Martin, R. L. *J. Chem. Soc., Dalton Trans.* **1979**, 92.

(31) Mackey, D. J.; Martin, R. L. *J. Chem. Soc., Dalton Trans.* **1978**, 702.

(32) Vos, G.; de Kok, A. J.; Verschoor, G. C. *Z. Naturforsch., B: Anorg. Chem., Org. Chem.* **1981**, *36B*, 809.

(33) Because of the variety of symbols and abbreviations used in susceptibility expressions by several authors, we prefer to give the expression used explicitly.

(34) The results of a Heisenberg fit of the magnetic data of the Co trimer ($S' = 1/2$) are given in Table VI to enable a comparison with $\text{Co}_3(\text{detrH})_6(\text{NCS})_6(\text{H}_2\text{O})_2$.

(35) For the procedure followed, see: Bonner, J. C.; Kobayashi, H.; Tsujikawa, I.; Nakamura, Y.; Friedberg, S. A. *J. Chem. Phys.* **1975**, *63* (1), 19.

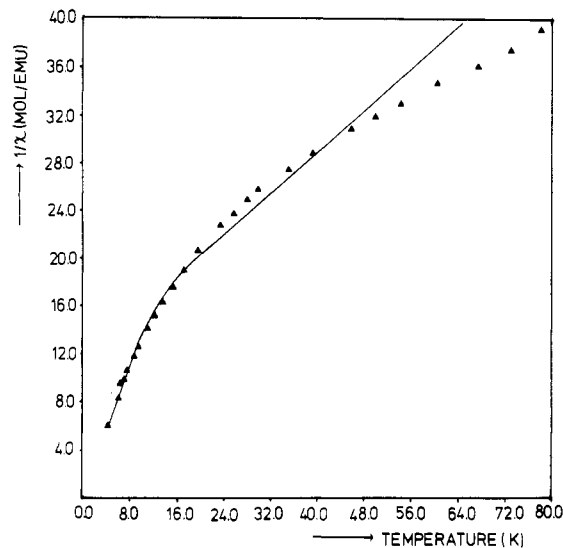


Figure 3. Plot of the reciprocal magnetic susceptibility ($1/\chi$) vs. temperature for $[\text{Co}_3(\text{detrH})_6\text{F}_2(\text{NCS})_4](\text{H}_2\text{O})_2$. The drawn curve is the theoretical prediction of a linear Ising trimer with $g_{\parallel} = 8.23$ (4) and $J_{\parallel} = -17.4$ (7) cm^{-1} (diamagnetic correction = -223×10^{-6} emu/Co).

eigenvalues in the well-known Van Vleck equation³⁶ results in the following expression for χ_{\parallel} :

$$\chi_{\parallel, \text{M}} = \frac{N_A g_{\parallel}^2 \mu_B^2}{4kT} \frac{2 + e^{-x} + 9e^x}{2 + e^{-x} + e^x} \quad x = J_{\parallel}/kT \quad (2)$$

Since this expression refers to 1 mol of the compound, it is necessary to divide by 3 to obtain χ_{\parallel} per mole of Co: $\chi_{\parallel, \text{A}} = 1/3 \chi_{\parallel, \text{M}}$. A validity check by insertion of $x = 0$ (vide supra) yields $\chi_{\parallel, \text{A}} = N_A g_{\parallel}^2 \mu_B^2 / 4kT$; this is exactly the spin-only expression according to the Curie law for $S = 1/2$. For a powder, one should have $\chi_{\text{powder}} = (2\chi_{\perp} + \chi_{\parallel})/3$; consequently, with χ_{\perp} set to zero, the magnetic susceptibility data were fitted to eq 3. Simultaneous variation

$$\chi_{\text{powder}} = 1/3 \chi_{\parallel, \text{A}} = \frac{N_A g_{\parallel}^2 \mu_B^2}{36kT} \frac{2 + e^{-x} + 9e^x}{2 + e^{-x} + e^x} \quad (3)$$

of J_{\parallel} and g_{\parallel} (weights $w_i = 1$) yielded $J_{\parallel} = -17.4$ (7) cm^{-1} and $g_{\parallel} = 8.23$ (4). In Figure 3, $1/\chi$ is shown as a function of T . The solid curve is the theoretical prediction of $1/\chi_{\text{powder}}$ according to the Ising model with an effective spin of $1/2$, assuming that χ_{\perp} is negligible. It is clearly seen from Figure 3 that the fit of the data to the Ising equation derived is not satisfactory. However, this is hardly surprising, if one realizes that the validity of eq 3 not only depends on the spin- $1/2$ assumption and the neglect of χ_{\perp} but also on the relative orientation of the z axes of the Co octahedra in the trimer. In fact, the Ising Hamiltonian used is only correct if the g tensors of the individual Co ions are collinear in the (arbitrarily) chosen coordinate system. The crystal structure implies that the trimer studied does not meet this requirement (because of the distortion of the octahedra of the terminal Co ions).

In view of the structural relationship between the fluoride-bridged trimers and the analogous NCS⁻-bridged compounds containing 3,5-diethyl-1,2,4-triazole,¹⁶ the difference in magnetic properties is remarkable (Table VI). The exchange interaction in the fluoride-bridged Ni trimer studied here is antiferromagnetic; the N-bridging thiocyanate analogue however shows an appreciable ferromagnetic exchange coupling ($J = +9.6 \text{ cm}^{-1}$). Although the exchange constants obtained for the related Co compounds are less reliable because of the fitting problems, clearly the fluoride-bridged Co compound shows a stronger antiferromagnetic exchange interaction than its NCS⁻ analogue. Because the exchange interaction is likely to proceed via the bridging anion, it is tempting to try to correlate the magnetic data to the M-X-M angle (X is the bridging anion). The Ni-X-Ni angle in $\text{Ni}_3(\text{detrH})_6(\text{NCS})_6(\text{H}_2\text{O})_2$ is 105.5° , while the corresponding angle in $\text{Ni}_3(\text{detrH})_6\text{F}_2(\text{NCS})_4(\text{H}_2\text{O})_2$ will be close to 114.4° (the value of the angle in the Co trimer; see Table IV). For dimeric compounds with single and double bridges (e.g. hydroxide, chloride) the effects of the bridging angle and the electronegativity of the bridging anion have been extensively studied.¹⁻⁶ The general trend is that both a larger bridging angle M-X-M and an increase in electron density on the bridging atom enhance the antiferromagnetic coupling. The same trend is visible in the trimeric compounds studied here: the combination of an increased electron density in the anionic bridge (because of the larger electronegativity of fluorine compared to nitrogen) and a larger bridging angle results in a larger AFM coupling in the fluoride-bridged compounds. However, because trimeric compounds containing triazole bridges only are also known to exhibit (weak) exchange coupling,²⁵ it seems risky to ascribe the observed interactions to the bridging anions only.

Concluding Remarks

The results described in the present paper show that fluoride anions can be incorporated in a linear array of metal ions (Co, Mn, Ni) linked by double 3,5-diethyl-1,2,4-triazole bridges. The compounds obtained show a larger antiferromagnetic exchange coupling between neighboring metal ions than the corresponding end-on NCS⁻-bridged compounds (i.e., the J value shifts downward). Unfortunately, attempts to incorporate other bridging anions like hydroxide, acetate, azide, and chloride have failed so far. Recently, another series of fluoride-bridged trimers of general formula $\text{M}_3\text{F}_2\text{L}_4(\text{NCS})_4(\text{H}_2\text{O})_x$ ($x = 2-6$) was obtained by using the same synthetic procedure as described here; the ligands L used are 3,4,5-trisubstituted 1,2,4-triazoles. The magnetic properties of these compounds are now under investigation.

Acknowledgment. The authors are indebted to Drs. L. J. de Jongh, R. Prins, W. G. Haye, and A. J. Kinneging for helpful discussions. The investigation was supported by the Netherlands Foundation for Chemical Research (SON) with financial aid from the Netherlands Organisation for the Advancement of Pure Research (ZWO).

Registry No. $[\text{Mn}_3(\text{detrH})_6\text{F}_2(\text{NCS})_4]$, 98064-58-5; $[\text{Co}_3(\text{detrH})_6\text{F}_2(\text{NCS})_4](\text{H}_2\text{O})_2$, 98087-67-3; $[\text{Ni}_3(\text{detrH})_6\text{F}_2(\text{NCS})_4]$, 98064-59-6.

Supplementary Material Available: Tables VII-X, listing anisotropic thermal parameters, additional bond lengths and angles, hydrogen atom positions, and observed and calculated structure factors for $\text{Co}_3\text{F}_2(\text{detrH})_6(\text{NCS})_4(\text{H}_2\text{O})_2$ (15 pages). Ordering information is given on any current masthead page.

(36) Van Vleck, J. H. "The Theory of Electric and Magnetic Susceptibilities"; Oxford University Press: London, 1932.